Noise and repeatability of airborne gravity gradiometry

Asbjorn Norlund Christensen[1*], Mark H. Dransfield[2] and Christopher Van Galder[2] present various noise estimates derived from surveys over the R.J. Smith Airborne Gravity Gradiometry Test Range in Western Australia.

For the past 15 years airborne gravity gradiometry has been used on a variety of petroleum and mineral exploration plays. As explorers focus on increasingly deeper targets with ever more subtle geophysical signatures, there is a growing need to accurately gauge the accuracy and resolution of airborne gravity gradiometer systems. In this article we present various noise estimates derived from surveys over the R.J. Smith Airborne Gravity Gradiometry Test Range in Western Australia.

Noise and resolution of AGG data

The first gravity gradiometer instrument to be used in airborne exploration was the FALCON Airborne Gravity Gradiometer (AGG). The AGG was designed and built explicitly for airborne use. Since 2005 the AGG has used fully digital electronics, making it smaller and lighter than other gravity gradiometers, and permitting its installation in smaller aircraft, particularly helicopters.

The AGG has one double-complement gravity gradiometer instrument mounted on a large wheel rotating slowly about a near-vertical axis within rotationally stabilized gimbals. The AGG simultaneously records two measurements of each of the horizontal curvature tensor components, G_{NE} and $G_{UV} = (G_{NN}-G_{EE})/2$, modulated at twice the rotation rate of the wheel.

The principal processing steps to be applied to the observed AGG data are correction for residual aircraft acceleration effects, followed by demodulation and filtering of the modulated tensor components. The limiting post-demodulation filtering is typically achieved with a Butterworth low-pass filter with a cut-off frequency at 0.18 Hz. At the nominal fixed-wing survey ground speed of 55m/s this corresponds to a spatial cut-off wavelength, λ_c, of 300 m. As the spatial resolution of the AGG data equals half the filter wavelength, the standard resolution of fixed-wing AGG data is 150 m.

The choice of cut-off wavelength presents a compromise between seeking to minimize the noise and seeking to maintain the spatial resolution in the data. Ideally, both the noise and the resolution should be small. However, the two are related and a trade-off exists. For normally distributed noise, the RMS value of the noise decreases when the data are filtered with a longer wavelength filter. Filtering decreases the noise but is detrimental to the resolution. To put it the other way around, improving the resolution increases the noise. The noise changes in proportion to the inverse square root of the filter wavelength. Equivalently, we can say that the product of the RMS noise, N_{RMS}, and the square root of the filter wavelength, $\sqrt{\lambda_c}$, is a constant.

$$N_{RMS} * \sqrt{\lambda_c} = C \quad (1)$$

This constant, C, called the *noise amplitude density* [Eö√km], describes the capability of the instrument and is useful for comparing the performance of different gravity gradiometers on moving platforms. However, the noise amplitude density is less useful for assessing the quality of acquired survey data. For interpretation purposes, it is necessary to know both the RMS noise and the resolution in order to be able to discriminate noise from signal. Specifying RMS noise only is poor practice (Dransfield and Christensen, 2013).

Following the demodulation and filtering process a number of deterministic corrections are applied to the observed data; these include corrections for the gravitational effects of the aircraft frame and platform masses as well as terrain corrections. Terrain corrections are calculated by forward modelling the gravity gradients from the high-resolution Digital Elevation Model (DEM) constructed from the laser scanner data.

Finally, the horizontal curvature tensor components are transformed to the remaining tensor components, including, most usefully, the vertical gravity gradient, G_{DD}, and to the vertical gravity, g_D. These transformations are performed by integration techniques (both in the spatial and wave-number domains) and by equivalent source techniques (Dransfield and Lee, 2004).

The R.J. Smith test ranges

The R.J. Smith Airborne Gravity and Airborne Gravity Gradiometry test ranges are located 115 km ENE from Perth's Jandakot airport in Western Australia (Howard et al.,

[1] *Nordic Geoscience.*
[2] *CGG.*
[*] *Corresponding author, E-mail: asbjorn_n_christensen@yahoo.com*

2010). The sites were established in 2009 as a benchmark for testing established and emerging airborne gravity and airborne gravity gradiometry technologies against a comprehensive high-resolution ground gravity data set.

The sites are located in a farming region around the hamlet of Kauring with gently rolling hills with some erosional incisions and an overall topographic relief of 115 m.

An outer 25 km by 25 km area has been surveyed extensively with ground gravity at 500 m by 500 m station spacing. This provides a test bed for airborne gravity systems, which typically have a minimum spatial resolution in excess of 1500 m full wavelength. Within the central part of the airborne gravity test range, a smaller 5 km by 5 km airborne gravity gradiometry test range has been established with ground gravity at a station spacing decreasing from 100 m by 250 m, in the northern and southern periphery, to 50 m by 50 m station spacing in the central part of the airborne gravity gradiometry test range (Figure 1). The variable station spacing is designed to accommodate both fixed-wing and helicopter-borne AGG systems, of which the fixed-wing AGG system has spatial resolution of 150 m and the helicopter-borne AGG system has a spatial resolution of 50 m (Dransfield, 2007).

Data acquisition and processing

CGG (then Fugro Airborne Surveys) flew the fixed-wing AGG system in a Cessna 208 Grand Caravan over the R.J. Smith Airborne Gravity Gradiometry Test Range over three periods in July 2011, November 2011 and February 2012. These were the first test flights of the newly commissioned second-generation digital AGG system, FALCON-II. The purpose of the surveys was to assess and demonstrate the accuracy of the AGG system against the high-resolution, public domain, ground gravity data set. The site was flown with 50 m line spacing and 1000 m tie-line spacing as a draped survey with a nominal terrain clearance of 70 m (Figure 1).

The transformation of the measured G_{NE} and G_{UV} gravity gradient components to vertical gravity, g_D, and vertical gravity gradient, G_{DD}, was performed by standard potential field Fourier integration and derivative techniques on to the aircraft drape surface. The AGG data and the ground gravity data have been fully terrain-corrected with a terrain density of 2.67 g/cm^3.

In order to effectively compare the AGG vertical gravity, g_D, with the vertical ground gravity, it is necessary to upward continue the vertical ground gravity from the ground surface to the aircraft drape surface.

Likewise, in order to compare the AGG vertical gravity gradient, $G_{DD,}$ data with the computed vertical gradient ground gravity, it is necessary to upward continue the vertical gradient ground gravity from the ground surface to the aircraft drape surface.

A wavenumber-domain method to effectively upward continue potential field data between two arbitrary surfaces by means of equivalent sources has been proposed by Xia et al. (1993). We have used the USGS software implementation of this method (Phillips, 1996; 1997) in the work presented here.

Noise estimates by data differencing.

The AGG is a double complement system which simultaneously records two measurements of each of the two horizontal curvature tensor components, (G_{NE}^{A}, G_{NE}^{B}) and (G_{UV}^{A}, G_{UV}^{B}). Analysis of the difference between the two observations of each of the two tensor components, ($G_{NE}^{A} - G_{NE}^{B}$) and ($G_{UV}^{A} - G_{UV}^{B}$), provides an immediate measure of the performance of the AGG system.

The turbulence for the survey was moderate, yet average RMS difference noise levels in the measured G_{NE} and G_{UV} gravity gradiometer component data were only 2.3 Eö. Simple white noise in G_{NE} and G_{UV} transforms to white noise in G_{DD} at twice the amplitude, so we can conservatively estimate the AGG G_{DD} noise as double the reported values of horizontal curvature component noise (Dransfield and Christensen, 2013). Hence, this suggests that the vertical gravity gradient G_{DD} has an RMS error of 4.6 Eö at 300 m full wavelength low-pass filtering. This is equivalent to a noise amplitude density of 2.5 Eö√km. This estimate is probably too low, as noise estimated from difference values does not capture coherent noise in the horizontal curvature tensor components.

Noise estimates by comparison with ground gravity data

A map of the AGG vertical gravity gradient, G_{DD}, is shown in Figure 2 (a). The central part of the R.J. Smith Airborne Gravity Gradiometry Test Range is host to a distinct vertical gravity gradient anomaly exceeding 80 Eö at the northern limit of a NW-NNW striking linear vertical gravity gradient high. For comparison, Figure 2 (b) also shows a map of the corresponding vertical gradient of the vertical ground gravity, as derived from the original vertical ground gravity data and subsequently variably upward continued to the aircraft drape surface by the equivalent source method (Xia et al., 1993). Both data sets have been low-pass filtered with a 2nd order Butterworth filter with a cut-off wavelength of 300 m.

There is good correspondence between the AGG vertical gravity gradient, G_{DD}, and the corresponding upward continued vertical gradient of the vertical ground gravity; not only along the high-amplitude central structure, but also with more subtle NE-SW trending features of lesser amplitude. This general correspondence is reflected in the map in Figure 2 (c) showing the difference between the AGG vertical gravity gradient, G_{DD}, and the corresponding upward continued vertical gradient of the vertical ground gravity. The range of the difference map is [-24 Eö, 27 Eö], the mean is 0.0 Eö and the standard deviation of the difference map is 5.6 Eö at 300 m full wavelength low-pass filtering. This is equivalent to a noise amplitude density of 3.1 Eö√km. This

estimate is probably too high, as it not only captures the noise of the AGG system, but also includes the noise inherent in the ground gravity data (Christensen, 2013).

A map of the AGG vertical gravity, g_D, is shown in Figure 2 (d). The central anomaly in the Airborne Gravity Gradiometry Test Site corresponds to a vertical gravity anomaly exceeding 1.6 mGal. For comparison, Figure 2(e) shows a map of the corresponding vertical ground gravity variably upward continued to the aircraft drape surface, again by the wavenumber-domain equivalent source method. Both data sets have had any first order trend removed.

Again, there is good correspondence between the AGG vertical gravity, g_D, and the corresponding variably upward continued vertical ground gravity. This general correspondence is also reflected in Figure 2 (f) showing the difference between the AGG vertical gravity, g_D,

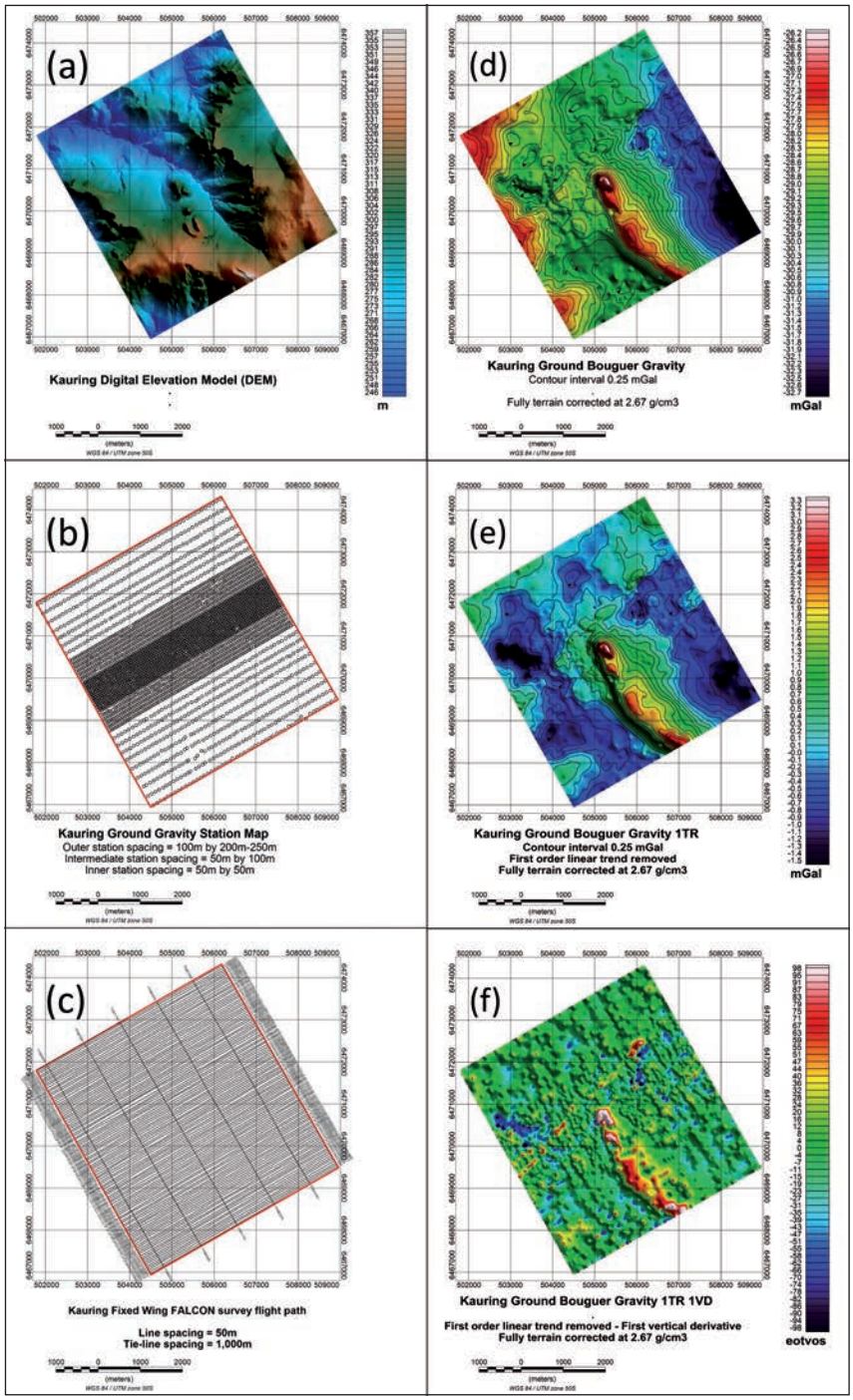

Figure 1 *(a) Map of the Digital Elevation Model (DEM) over the R.J. Smith Airborne Gravity Gradiometry Test Range. (b) Ground gravity stations. (c) Fixed-wing AGG survey flight path. (d) Bouguer and terrain-corrected ground gravity. (e) Residual ground gravity data after removal of a bilinear trend in (d). (f) Vertical-gradient filtered residual ground gravity data.*

and the corresponding upward continued vertical ground gravity. The range of the difference map is [-0.52 mGal, 0.58 mGal], the mean is 0.0 mGal and the standard deviation of the difference map is 0.18 mGal.

Noise estimates from repeat flying

The R.J. Smith Airborne Gravity Gradiometry test range was fully surveyed by the AGG system in July 2011. One part of the test site was reflown in November 2011, and another in February 2012, for further instrument testing purposes. The repeat flying allows us to analyse the repeatability of the AGG system (Christensen and Dransfield, 2014). A map of the AGG vertical gravity gradient, G_{DD}, from surveying in July 2011 is shown in Figure 3 (a). For comparison, Figure 3 (b) shows a map of the AGG vertical gravity gradient, G_{DD}, from repeat surveying in November 2011

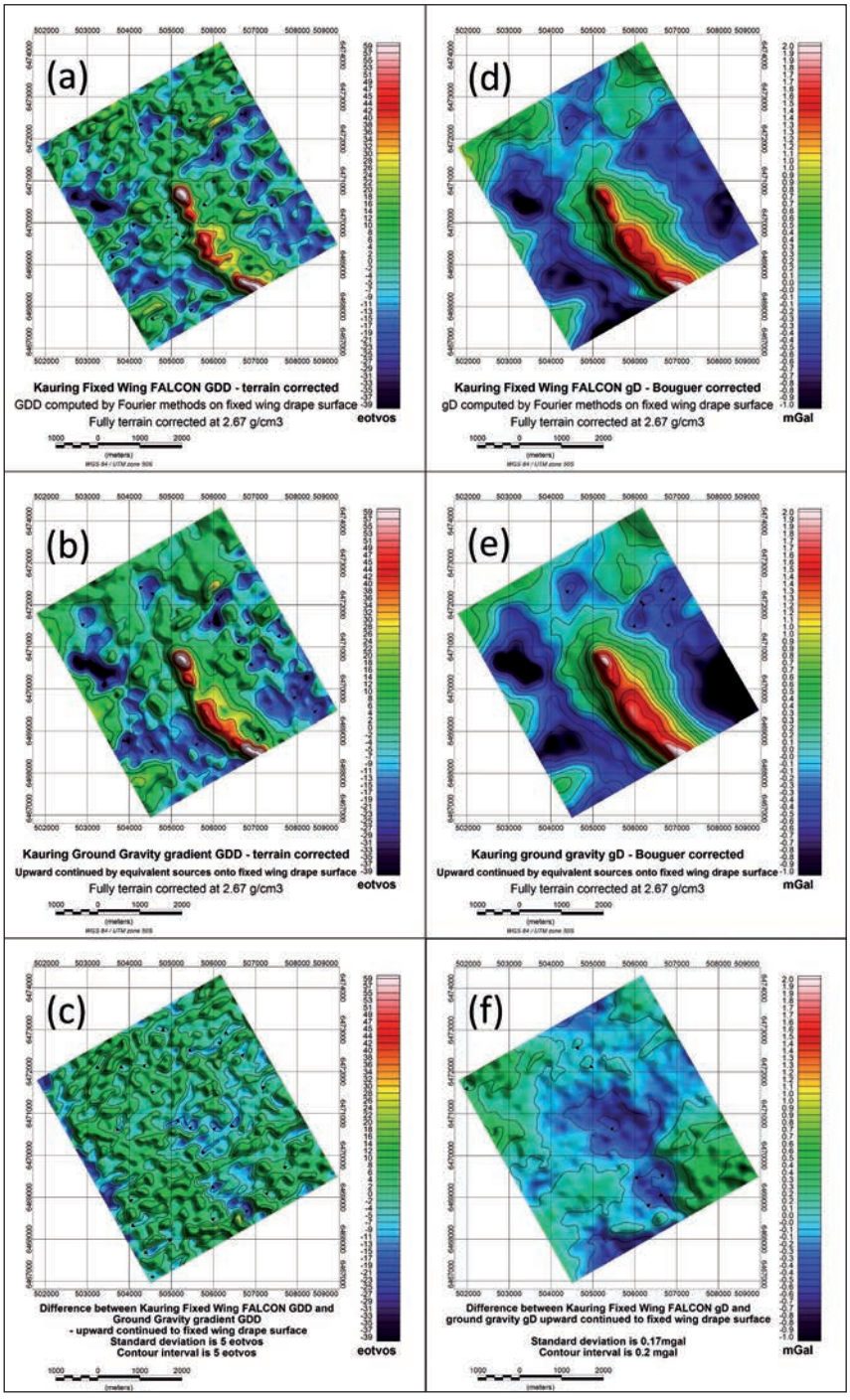

Figure 2 *(a) AGG G_{DD} vertical gravity gradient, low-pass filtered at a cut-off wavelength of 300 m. (b) Vertical gradient filtered residual ground gravity, low-pass filtered at a cut-off wavelength of 300 m, and variably upward continued to the aircraft drape surface. (c) Difference between the AGG G_{DD} vertical gravity gradient and the upward continued vertical gradient filtered ground gravity. The standard deviation of the difference map is 5.6 Eö. (d) AGG g_D vertical gravity, low-pass filtered at a cut-off wavelength of 300 m. (e) Ground gravity, low-pass filtered at a cut-off wavelength of 300 m and variably upward continued to the aircraft drape surface. (f) Difference between the AGG g_D vertical gravity and the upward continued ground gravity. The standard deviation of the difference map is 0.18 mGal.*

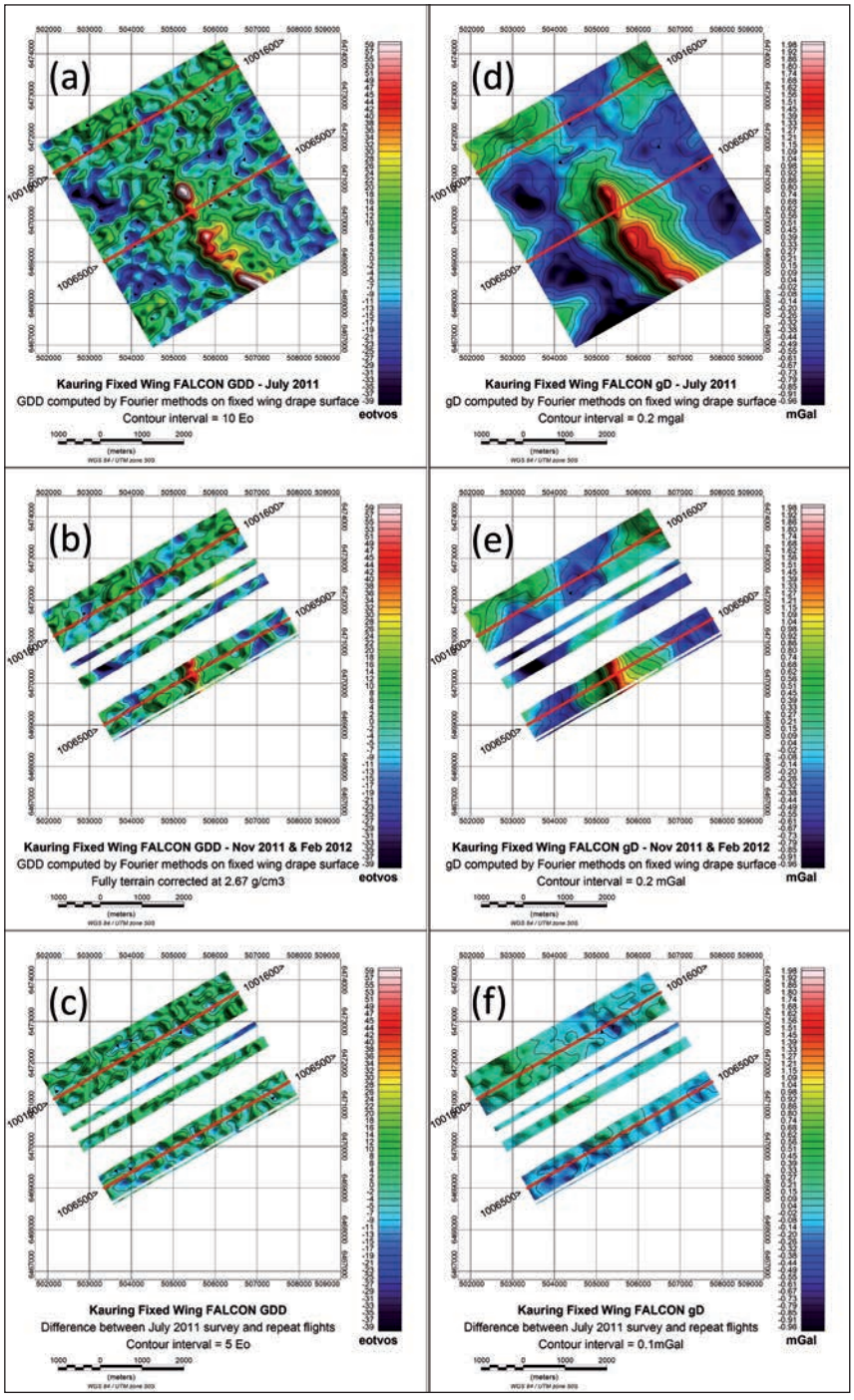

Figure 3 *(a) AGG G_{DD} vertical gravity gradient from surveying in July 2011. (b) AGG G_{DD} vertical gravity gradient from repeat surveying in November 2011 and February 2012. (c) Difference between the AGG G_{DD} vertical gravity gradient data from the July 2011 survey and the repeat surveying. The standard deviation of the difference is 4.7 Eö. (d) AGG g_D vertical gravity from surveying in July 2011. (e) AGG g_D gravity from surveying in July 2011. (e) AGG g_D gravity from repeat surveying in November 2011 and February 2012. (f) Difference between the AGG g_D gravity data from the July 2011 survey and the repeat surveying. The standard deviation of the difference is 0.1 mGal.*

and February 2012. In addition, Figure 3 (c) shows a map of the difference between the AGG G_{DD} vertical gravity gradient data from the July 2011 survey and the repeat surveying in November 2011 and February 2012. The range of the difference map is [-21 Eö, 19 Eö]. The mean difference is 0.2 Eö, and the standard deviation of the difference map is 4.7 Eö at 300 m full wavelength low-pass filtering. This is equivalent to a noise amplitude density of 2.5 Eö√km. This estimate may be too high, as it also includes variations in the flight trajectories in different sorties. A similar analysis on the AGG vertical gravity, g_D, Figure 3 (d), yields a difference map between the AGG g_D vertical gravity data from the July 2011 survey and the repeat surveying, Figure 3 (f). The range of the difference map is [0.26 mGal; 0.33m Gal]. The mean difference is 0.01 mGal, and the standard deviation of the difference map is 0.10 mGal.

Figure 4 (a) shows a profile of flight trajectories along line 65 over the terrain from surveying in July 2011 (Flight 4) and from repeat surveying in November 2011 (Flight 27). Figure 4 (b) shows a profile section along survey line 65 of AGG vertical gravity gradient, G_{DD}, from surveying in July 2011 (Flight 4) and from repeat surveying in November 2011 (Flight 27). The vertical ground gravity gradient – upward continued to Flight 4 drape – is also shown with a +/- 5 Eö error bar range. Figure 4 (c) shows a profile section along survey line 65 of AGG g_D vertical gravity from initial surveying and from repeat surveying. Vertical ground gravity – upward continued to initial survey drape – is shown with a +/- 0.20 mGal error bar range.

Improving the resolution

Although the directly measured horizontal curvature tensor components, G_{NE} and G_{UV}, are unaffected by line spacing, the transformation to vertical gravity (g_D) and its vertical gradient (G_{DD}) does impose requirements on sampling. For mineral exploration surveys traverse line spacing of 100-400m is common, and here a spatial cut-off wavelength of 300 m provides a good balance between low noise and acceptable lateral resolution.

However, if a fixed-wing AGG survey is acquired with traverse line spacing equal to or less than 100 m, then the cut-off wavelength can be reduced and the resolution improved (Christensen et al., 2014).

In order to demonstrate that the tighter line spacing will allow for shorter low-pass filtering, the AGG data was reprocessed at 100 m traverse line spacing with the post-demodulation low-pass filtering at a spatial cut-off wavelength of only 100 m.

A map of the AGG vertical gravity gradient, G_{DD}, low-pass filtered at a cut-off wavelength of 100 m, is shown in Figure 5 (a). For comparison, Figure 5 (b) also shows a map of the corresponding vertical gradient filtered ground gravity, low-pass filtered at a cut-off wavelength of 100 m and variably upward continued to the aircraft drape surface. Figure 5 (c) shows the difference between the AGG vertical gravity gradient, G_{DD}, low-pass filtered at a cut-off wavelength of 100 m, and the corresponding upward continued vertical gradient of the ground gravity. The range of the difference map is [-52 Eö, 43 Eö], the mean is 0.0 Eö and the standard deviation of the difference map is 8.3 Eö. As the cut-off wavelength is 100 m, the corresponding noise amplitude density is 2.6 Eö√km.

Inspection of the difference map in Figure 5 (c) reveals an element of striping in the inline and cross line directions. These are predominantly levelling and gridding artifacts, which are normally removed in standard processing. These were largely eliminated by applying a tapered low-pass inline and cross line directional-rejection filter to the grids of the horizontal curvature components of the gravity gradient, G_{NE} and G_{UV}, prior to the transformation to g_D and G_{DD}. The power spectrum of the tapered low-pass inline and cross line directional-rejection filter is shown in Figure 6.

A map of the directional-rejection filtered vertical gravity gradient, G_{DD}, is shown in Figure 5 (d). For comparison, Figure 5 (e) also shows a map of the corresponding vertical gradient of the ground gravity.

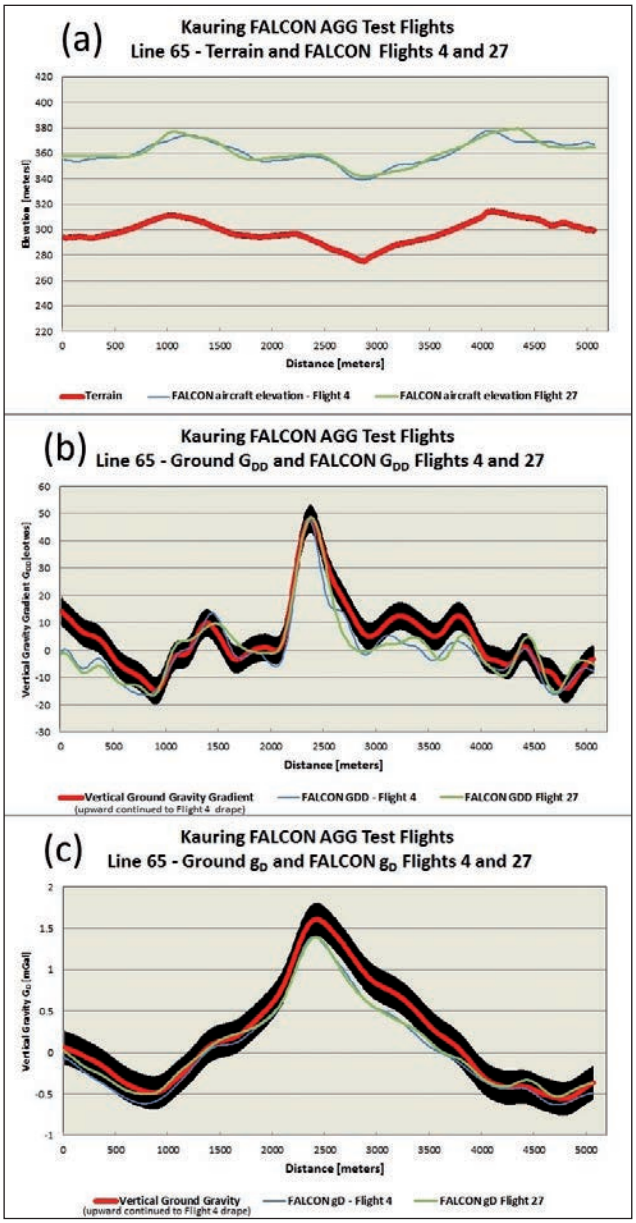

Figure 4 *(a) Profile of flight trajectories along line 65 over DEM (red) from surveying in July 2011 (Flight 4) and from repeat surveying in November 2011 (Flight 27). (b) Profile of AGG G_{DD} vertical gravity gradient from surveying in July 2011 (Flight 4) and from repeat surveying in November 2011 (Flight 27). Vertical ground gravity gradient – upward continued to Flight 4 drape – is shown with a +/- 5 Eö error bar range. (c) Profile of AGG g_D vertical gravity from surveying in July 2011 (Flight 4) and from repeat surveying in November 2011 (Flight 27). Vertical ground gravity – upward continued to Flight 4 drape - is shown with a +/- 0.20 mGal error bar range.*

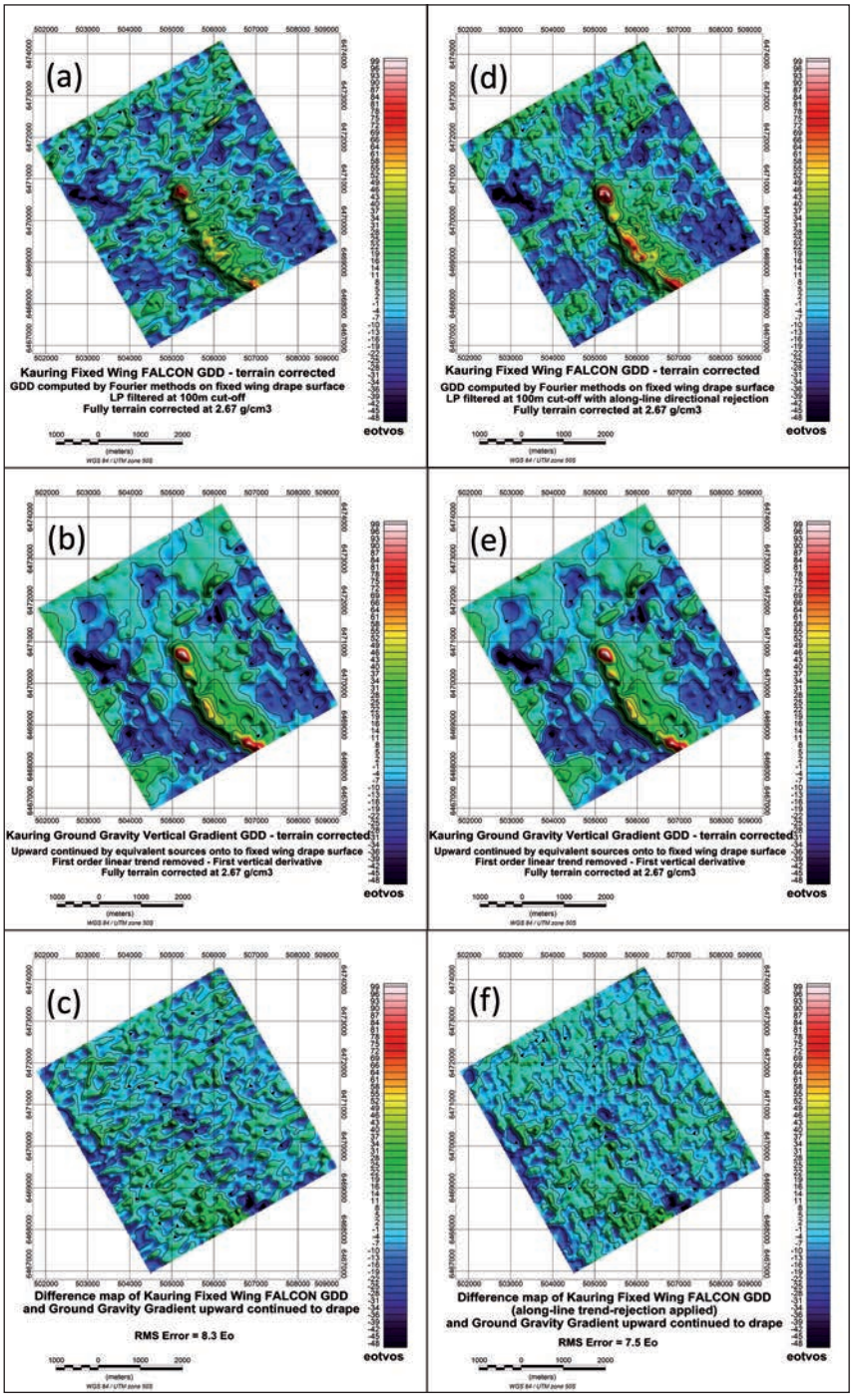

Figure 5 *(a) AGG G_{DD} vertical gravity gradient data, low-pass filtered at a cut-off wavelength of 100 m. (b) Vertical gradient of filtered ground gravity, low-pass filtered at a cut-off wavelength of 100 m, variably upward continued to the aircraft drape surface, (c) Difference between the AGG G_{DD} vertical gravity gradient and the upward continued vertical gradient filtered ground gravity. The standard deviation of the difference is 8.3 Eö. (d) AGG G_{DD} vertical gravity gradient data, low-pass filtered at a cut-off wavelength of 100 m with directional-rejection filtering applied. (e) Vertical gradient filtered ground gravity, low-pass filtered at a cut-off wavelength of 100 m, variably upward continued to the aircraft drape surface, (f) Difference between the AGG G_{DD} vertical gravity gradient with directional-rejection filtering applied and the upward continued vertical gradient filtered ground gravity. The standard deviation of the difference is 7.5 Eö.*

There is very good correspondence between the directional-rejection filtered vertical gravity gradient, G_{DD}, and the corresponding upward continued vertical gradient of the vertical ground gravity; not only along the high-amplitude central structure, and with the more subtle NE-SW trending features of lesser amplitude, but also among the lower-amplitude lows and highs surrounding the central structure.

Figure 5 (f) shows the difference map between the directional-rejection filtered vertical gravity gradient, G_{DD}, and the corresponding upward continued vertical gradient of the ground gravity. The range of the difference map is [-44 Eö, 47 Eö], the mean is 0.0 Eö and the standard deviation of the difference map is 7.5 Eö. As the cut-off wavelength is 100 m, the corresponding noise amplitude density is 2.4 Eö√km.

Conclusions

Subsequent to the surveys flown over the R.J. Smith Airborne Gravity Gradiometry Test Range in Western Australia, our estimates of accuracy and resolution of the airborne gravity gradiometer indicate that at 300 m low-pass filtering the system has a vertical gravity g_D error of less than 0.1 mGal, and a vertical gravity gradient G_{DD} error of less than 4.7 Eö. The main results are summarized below and in Table 1.

Direct analysis of the difference noise of the observed horizontal curvature components indicates that the AGG G_{DD} component has an error of 4.6 Eö at 300 m full wavelength low-pass filtering. This is equivalent to a noise amplitude density of 2.5 Eö√km. This estimate may be too low, as it does not include any correlated noise in the observed horizontal curvature components.

Comparison between the AGG survey data and the high-resolution ground gravity data over the R.J. Smith Airborne Gravity Gradiometry Test Range indicates that the AGG vertical gravity, g_D, has an error of 0.18 mGal, and that the AGG vertical gravity gradient G_{DD} has an error of 5.6 Eö at 300 m full wavelength low-pass filtering. This is equivalent to a noise amplitude density of 3.1 Eö√km. This estimate is probably too high, as it includes the noise inherent in the ground gravity data.

Analysis of repeat surveying over the R.J. Smith Airborne Gravity Gradiometry test range suggests slightly lower errors of the order of 0.10 mGal for the AGG vertical gravity, g_D; and that the AGG vertical gravity gradient G_{DD} has an error of +/- 4.7 Eö at 300 m full wavelength low-pass filtering. This is equivalent to a noise amplitude density of 2.5 Eö√km. This estimate may be too high, as it also includes variations in the flight trajectories in different sorties.

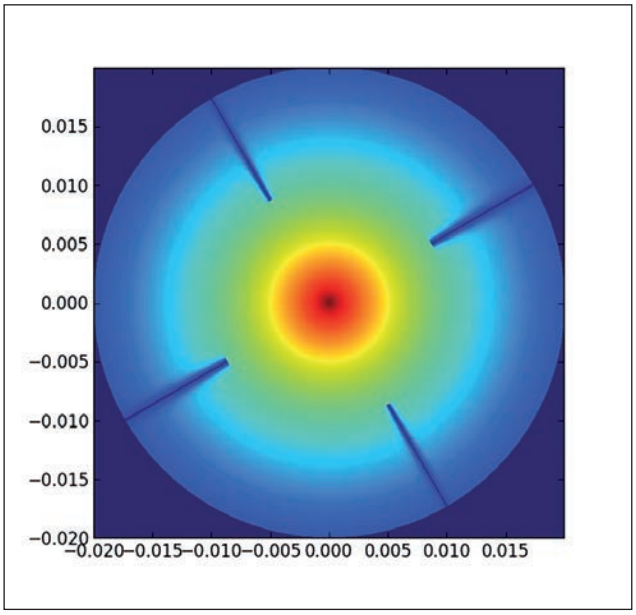

Figure 6 *Power spectrum of the tapered low-pass inline and cross line directional-rejection filter.*

We have demonstrated that for fixed-wing AGG surveys flown with a traverse line spacing equal to or less than 100 m the post-demodulation low-pass filter cut-off wavelength can be reduced from the normal 300 m to 100 m only, resulting in a 50 m resolution of the G_{DD} data. The 66% improvement in resolution (from 150 m to 50 m) is accompanied by 50% higher RMS noise levels in the data (from 5.6 Eö to 8.3 Eö). As some of the noise is coherent in specific acquisition-dependent directions, careful line levelling and directional rejection filtering (micro-levelling) can reduce the RMS noise increase to only 30% (from 5.6 Eö to

Noise Measure Method	Estimated g_D RMS noise with 300m low-pass filtering	Estimated G_{DD} RMS noise with 300m low-pass filtering	Estimated Noise Amplitude Density	Comment
Instrument Difference	N/A	4.6 Eö	2.5 Eö√km	This noise estimate may be too low, as it does not include any correlated noise.
Repeat Surveying	0.1 mGal	4.7 Eö	2.5 Eö√km	This noise estimate may be too high, as it also includes variations in the flight trajectories in different sorties.
Comparison with Ground Gravity	0.18 mGal	5.6 Eö	3.1 Eö√km	This noise estimate is probably too high, as it includes the noise inherent in the ground gravity data.

Table 1 *Summary of AGG noise estimates derived from the surveys flown over the R.J. Smith Airborne Gravity Gradiometry Test Range.*

7.5 Eö). As the cut-off wavelength is 100 m, the corresponding noise amplitude density is 2.5 Eö√km.

The insights gained from flying the newly commissioned second-generation FALCON-II system over the R.J. Smith Airborne Gravity Gradiometry Test Range has subsequently resulted in an estimated 50% reduction in AGG survey noise, as G_{NE} and G_{UV} noise levels at 1.35 Eö RMS at 300 m full wavelength low-pass filtering have been reported (Moore et al., 2012). This is equivalent to a G_{DD} noise amplitude density of 1.5 Eö√km.

The ground gravity data from the R.J. Smith Airborne Gravity Gradiometry Test Range and the AGG survey data are publicly available for download through the Airborne Geophysics Index (MAGIX) at the website of the Government of Western Australia – Department of Mines and Petroleum (http://www.dmp.wa.gov.au).

We strongly recommend the collection and publication of comparative analyses over the R.J. Smith Airborne Gravity Gradiometry test range and areas with similar-quality ground gravity data to establish the capability of all AGG systems.

Acknowledgements

We are grateful to the management of CGG for permission to publish this paper. Special thanks go to the data processing team at CGG Multi-Physics for all their work with the R.J. Smith Airborne Gravity Gradiometry test range data.

References:

Christensen, A.N. [2013] Results from FALCON® Airborne Gravity Gradiometer surveys over the Kauring AGG Test site. *ASEG Extended Abstracts,* **1**, 1–4.

Christensen, A.N. and Dransfield, M.H. [2014] Noise and Repeatability of Airborne Gravity Gradiometry. *76th EAGE Conference & Exhibition*, Extended abstracts.

Christensen, A.N., Van Galder, C. and Dransfield, M.H. [2014] Improved resolution of fixed wing airborne gravity gradiometer surveys. *SEG Technical Program*, Expanded Abstract, 1319-1323.

Dransfield, M. [2007] Airborne Gravity Gradiometry in the Search for Mineral Deposits. In: Milkereit, B. (Ed.) *Proceedings of Exploration 07. Fifth Decennial International Conference on Mineral Exploration*, 341-354.

Dransfield, M.H. and Christensen, A.N. [2013] Performance of airborne gravity gradiometers. *The Leading Edge*, **32**(8), 908–922.

Dransfield, M.H. and Lee, J.B. [2004] The FALCON airborne gravity gradiometer survey systems. In: Lane, R. (Ed.) *Airborne Gravity 2004 – Abstracts from the ASEG-PESA Airborne Gravity 2004 Workshop,* Geoscience Australia, 15-19.

Howard, D., Grujic, M. and Lane, R. [2010] The Kauring airborne gravity and airborne gravity gradiometer test site, Western Australia. In: Lane, R. (Ed.) *Airborne Gravity 2004 – Abstracts from the ASEG-PESA Airborne Gravity 2004 Workshop,* Geoscience Australia, 107-114.

Moore, D., Chowdhury, P.R. and Rudge, T. [2012] FALCON™ Airborne Gravity Gradiometry provides a smarter exploration tool for unconventional and conventional hydrocarbons: case study from the Fitzroy Trough, onshore Canning Basin. In: Mares, T. (Ed.) *Eastern Australasian Basins Symposium IV*, Petroleum Exploration Society of Australia, Special Publication, CD-ROM.

Phillips, J.D. [1996] Potential-field continuation: Past practice vs. modern methods. *SEG Technical Program Expanded Abstracts*, 1411-1414.

Phillips, J.D. [1997] Potential-field geophysical software for the PC, version 2.2. *U.S. Geological Survey Open-File Report 97-725*, 34.

Xia, J., Sprowlt, D.R. and Adkins-Heljeson, D. [1993] Correction of topographic distortions in potential-field data: A fast and accurate approach. *Geophysics*, **58**, 515-523.